2007-06-19

Optimization of nano-magneto-optic sensitivity using dual dielectric layer enhancement

Aaron R. Hawkins
hawkins@ee.byu.edu

J. D. Maas

S. Wang

A. Barman

Holger Schmidt

Original Publication Citation

Wang, S., A. Barman, H. Schmidt, J. D. Maas, A. R. Hawkins, S. Kwon, B. Harteneck, S. Cabrini, and J. Bokor. "Optimization of nano-magneto-optic sensitivity using dual dielectric layer enhancement." Applied Physics Letters 9 (27)

BYU ScholarsArchive Citation

Authors

Aaron R. Hawkins, J. D. Maas, S. Wang, A. Barman, Holger Schmidt, S. Kwon, B. Harteneck, S. Cabrini, and J. Bokor

Optimization of nano-magneto-optic sensitivity using dual dielectric layer enhancement

S. Wang,[a] A. Barman,[b] and H. Schmidt
School of Engineering, University of California, Santa Cruz, 1156 High Street, Santa Cruz, California 95064

J. D. Maas and A. R. Hawkins
ECEn Department, Brigham Young University, 459 Clyde Building, Provo, Utah 84602

S. Kwon,[c] B. Harteneck, S. Cabrini, and J. Bokor
Molecular Foundry, Lawrence Berkeley National Laboratory, Berkeley, California 94720

(Received 4 April 2007; accepted 25 May 2007; published online 19 June 2007)

We discuss maximization of the sensitivity of magneto-optical detection of single nanomagnets. We show that a combination of optimized dielectric coating on the magnets with an antireflection coated substrate can increase the areal magneto-optic sensitivity by about three orders of magnitude in the deep nanometer range. A dual layer nanofabrication process is developed to implement this approach, and magnetization switching of single nickel nanomagnets with 50 nm diameter is demonstrated. © *2007 American Institute of Physics*. [DOI: 10.1063/1.2750389]

The field of nanomagnetism has been fueled during the last decade by the development of sophisticated nanofabrication methods and potential applications in high areal density media and fast read/write heads of future magnetic data storage and spintronic devices.[1,2] Characterization of dynamic nanomagnet properties is of particular interest for high-speed device operation[3,4] and requires simultaneous high spatial and temporal resolutions. Magneto-optic Kerr effect (MOKE) microscopy is a well-known technique for studying ultrafast magnetization dynamics. MOKE has been used for studying the magnetization dynamics of both magnetic thin films,[5,6] patterned microscale magnets[7–9] and nanomagnet arrays.[10,11] However, array measurements include dipolar broadening and dynamic dephasing effects from the neighboring elements and prevent us from obtaining the intrinsic precession dynamics of individual nanomagnets, which suggests the requirement of nanoscale spatial resolution. It had been well known that an appropriate use of dielectric layers (cavity) enhances the magneto-optic signal due to multiple reflections off the magnetic layer.[12–14] More recently, cavity enhancement (CE) of MOKE has been applied to increase the spatial sensitivity of MOKE measurements on single nanomagnets without affecting the static or dynamic magnetic properties.[15–17] Both quasistatic switching[16] and picosecond magnetization precession[17] were observed using far-field optics for magnets with diameters on the order of 100 nm. In this letter, we explore the maximization of cavity enhanced far-field magneto-optical measurements on single nanomagnets by concurrent optimization of the magnetic surface and the surrounding substrate. A new nanofabrication process that is compatible with the optimization strategy is developed and implemented, and the improvement in resolution is demonstrated experimentally. Finally, the limits of far-field MOKE enhancement [magneto-optic enhancement (ME)] in the limit of small nanomagnets are determined.

The basic concept of previously implemented CE-MOKE is illustrated in Fig. 1(a). The sample under study is coated with a dielectric enhancement layer (EL) covering both the magnet and the substrate. By properly choosing the thickness and material index of the dielectric layer, one can improve the Kerr signal reflected off the magnetic surface through constructive multiple reflection. In far-field excitation, only the central part of an excitation beam with the Gaussian profile (spot size w_0) is reflected off the coated magnet surface (reflectivity R_{mag}), while the remaining part is reflected off the substrate (reflectivity R_{sub}). The resulting total Kerr angle can be described very well with a geometric

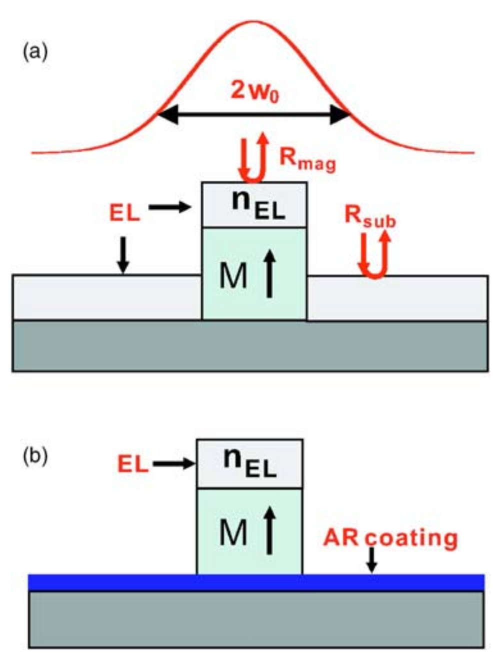

FIG. 1. (Color online) (a) Nanomagnets and substrate coated with an enhancement layer (EL) are excited with a Gaussian beam in the far field (spot size w_0). (b) AR coating on the substrate and EL (index n_{EL}) on top of the nanomagnet.

[a]Electronic mail: suqinw@soe.ucsc.edu
[b]Also at Department of Physics, Indian Institute of Technology Delhi, Haus Khas, New Delhi 110016, India.
[c]Also at School of Electrical Engineering, Seoul National University, Seoul 155-744, Korea.

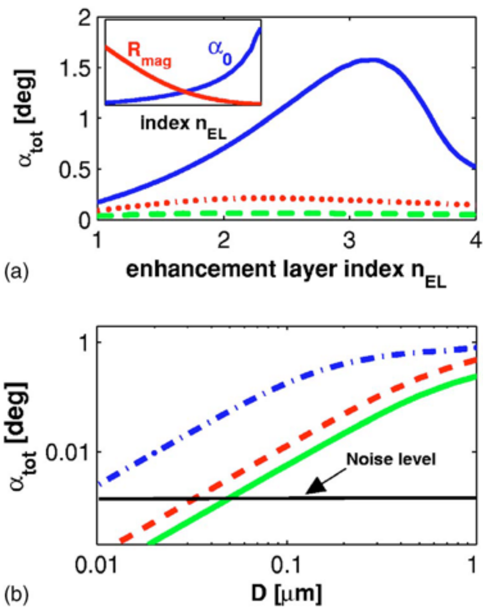

FIG. 2. (Color online) (a) Kerr angle vs enhancement layer index n_{EL} for various magnet diameters. Solid line: 500 nm, dotted line: 100 nm, dashed line: 50 nm, and inset: dependence of CE and R_{mag} on n_{EL}. (b) Kerr signal improvement for different sample configurations. Solid line: SiN coated everywhere, dashed line: optimized EL coating index, and dash-dotted line: index optimization and 0.2% AR coating on the substrate.

model.[16] For the polar MOKE geometry we used, the total relative ME factor is given by

$$\mathrm{ME} = \frac{\alpha_{tot}}{\alpha_0} = \frac{\mathrm{CE}}{1 + (R_{sub}/R_{mag})[e^{D^2/2w_0^2} - 1]^{-1}}, \tag{1}$$

where α_0 and α_{tot} are the magnet-intrinsic and total measurable Kerr angles, respectively, CE is the cavity enhancement factor, and D is the magnet diameter. The spatial sensitivity of the MOKE measurement is optimized by maximizing the total enhancement factor ME. All previous work had focused on maximizing the CE, but even better results can be obtained by optimizing all parts of Eq. (1).

The first strategy is to choose the enhancement layer index n_{EL} that maximizes α_{tot}. The total-Kerr angle depends on n_{EL} via both the CE factor and the magnet reflectivity R_{mag}, i.e., $\alpha_{tot}(n_{EL}) = \alpha_{tot}(\mathrm{CE}(n_{EL}), R_{mag}(n_{EL}))$. Figure 2(a) shows the calculated Kerr angle from nickel nanomagnets as a function of n_{EL} for various magnet diameters D and a substrate reflectivity of $R_{sub}=0.2\%$. We see that an optimum index $n_{EL,opt}$ exists for each diameter and that the value of $n_{EL,opt}$ decreases with D. To understand the existence of this maximum, we need to consider the total derivative of α_{tot} with respect to n_{EL}, which is given by

$$\frac{d\alpha_{tot}}{dn_{EL}} = \frac{\partial\alpha_{tot}}{\partial\mathrm{CE}}\frac{\partial\mathrm{CE}}{\partial n_{EL}} + \frac{\partial\alpha_{tot}}{\partial R_{mag}}\frac{\partial R_{mag}}{\partial n_{EL}}. \tag{2}$$

It can be seen from Eq. (1) that both partial derivatives of α_{tot} in Eq. (2) are positive, but the inset of Fig. 2(a) shows that CE increases with n_{EL} ($\partial\mathrm{CE}/\partial n_{EL}>0$) while R_{mag} decreases ($\partial R_{mag}/\partial n_{EL}<0$). This effect had been pointed out previously.[15] Consequently, the two terms on the right hand side of Eq. (2) have opposite signs resulting in a maximum enhancement at $n_{EL,opt}$, where $d\alpha_{tot}/dn_{EL}=0$. The observed peak position shift with magnet diameter is introduced by the D dependence of $\partial\alpha_{tot}/\partial\mathrm{CE}$ and $\partial\alpha_{tot}/\partial R_{mag}$. Due to the highly nonlinear dependence of various quantities on n_{EL}, it is not possible to give an explicit analytical expression for Eq. (2) and the optimum index has to be determined numerically, as in Fig. 2(a). The dashed line in Fig. 2(b) shows the expected effect of using an optimized enhancement layer index for each diameter D on the maximum measurable Kerr angle α_{tot} compared with previously measured nickel cylinders coated with SiN (solid line).[16] Note that different R_{sub} values will result in different optimization curves.

The second optimization strategy is to minimize R_{sub} with a substrate antireflection coating, as shown in Fig. 1(b). This minimizes the unwanted contribution from the substrate, keeping R_{sub}/R_{mag} in Eq. (1) small and compensating the effect of the reduction of R_{mag} with higher n_{EL}. This effect is rather dramatic, as shown by the dash-dotted line in Fig. 2(b), where an antireflection (AR) coating with 0.2% reflectivity was assumed instead of the measured 4.6% reflectivity for the solid line. The combined effect of index optimization and AR coating improves the signal by more than two orders of magnitude, especially for magnets below 100 nm. Therefore, the best strategy from a practical standpoint is to minimize R_{sub} as much as possible and then determine $n_{EL,opt}$ based on the observed R_{sub} value and the given size of the nanomagnets under study. This analysis shows that an optimization of MOKE enhancement (ME) needs to consider the optical properties of both magnets (CE, R_{mag}) and substrate (R_{sub}) simultaneously.

In previous studies of cavity enhancement, a cavity enhancement layer was deposited on the entire sample after nanofabrication of the magnets.[16] However, this approach does not work with the new optimization strategy as the CE layer would cover the antireflection coating on the substrate. In addition, the previously used plasma-enhanced chemical-vapor deposition (PECVD) cannot be carried out before lift-off because the PECVD temperature is too high for the photoresist to maintain good lift-off properties. Therefore, we modified the nanofabrication process by replacing the SiN layer with an electron beam deposited SnO_2 layer which is compatible with the dual layer optimization strategy. A silicon substrate was covered with an antireflection coating ($R_{sub}=0.2\%$ at 780 nm). Subsequently, cylindrical nanomagnets were defined in a polymethyl methacrylate (PMMA) resist using electron beam lithography, followed by electron beam deposition of a thin titanium adhesion layer, a magnetic nickel layer, and a 63 nm thick tin oxide (SnO_2) cavity enhancement layer. SnO_2 has an index similar to SiN and exhibits CE values up to 4.5, comparable with CE=5 for SiN. Finally, the PMMA resist was removed using a lift-off step, resulting in optically and magnetostatically isolated cylindrical nickel magnets. The cylindrical nickel magnets had heights of either 50 or 100 nm and diameters from 3 μm to 18 nm.

Figure 3 shows the experimental results for quasistatic magnetization switching measurements on a number of samples: nickel on silicon (asterisks), SiN-coated magnets and substrate (squares), nickel on AR-coated silicon (circles), and SnO_2-coated nickel on AR-coated Si (stars). The experimental setup used was a far-field polar MOKE configuration with a laser diode source (780 nm), microscope objective (numerical aperture=0.85), avalanche photodetector, and lock-in detection based on photoelastic modulation.[18] Figure 3 shows the measured Kerr angles versus magnet diameter with all data normalized to the Kerr angle of a large bare

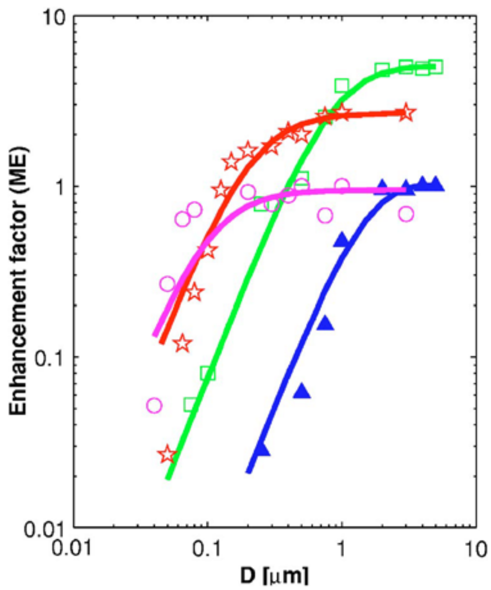

FIG. 3. (Color online) Experimental results and theory fitting to Eq. (1) (lines) for quasistatic magnetization switching measurements on different sample configurations: Bare nickel on silicon (asterisks), SiN-coated magnets and substrate (squares), nickel on AR-coated silicon (circles), and SnO_2-coated nickel on AR-coated Si (stars).

nickel magnet on silicon. Several trends are observed. All four samples show the characteristic MOKE signal drop for small magnet sizes.[16] However, the two optimization layers affect the unoptimized curve in different ways. Starting from the bare nickel magnet on silicon (asterisks), cavity enhancement (squares) leads to vertical displacement whereas the antireflection coating (circles) shifts the curve to the left. Both individual strategies result in a substantial improvement of the spatial sensitivity. The dual layer sample yields the largest signal down to a magnet size of 100 nm but is outperformed by the AR-coating-only sample below this value, which has the largest signal at $D=50$ nm. The reason for this finding is that the SnO_2 coating did not have the correct thickness resulting in a smaller than expected enhancement (CE$\sim$3 instead of 4.5). Therefore, the higher R_{mag} on bare Ni of the Ar-coating-only sample outweighs the CE effect of the dual layer sample. A higher CE value would have shifted the curve up more and resulted in a superior performance of the dual layer sample for all observed sizes. The solid lines in the figure represent fits to the data using Eq. (1) with the CE factor as fitting parameters. Overall, a very good agreement with the data is found, and, in particular, the crossover point between the dual layer and AR-coating-only curves is predicted correctly. Nevertheless, some discrepancies between experiment and theory are observed at the smallest dimensions. These could result from reduced reflection from the magnets due to nonideal surfaces or from differences between the nominal and actual magneto-optically active magnet diameter and shape. Finally, for the smallest dimensions the assumption of a bulk reflection coefficient from the magnet may start to break down, requiring the use of scattering theory for a more accurate description.

Given all the interdependencies between the experimental parameters, it is fair to ask what the ultimate limits of far-field MOKE enhancement are. For a setup-dependent detection limit $\alpha_{\min}$, the minimum detectable magnet diameter $D_{\min}$ can be found from Eq. (1) in the small magnet limit ($D \ll w_0$),

$$D_{\min} = \sqrt{\frac{\alpha_{\min}}{\alpha_0}\frac{2R_{\mathrm{sub}}w_0^2}{R_{\mathrm{mag}}}}. \quad (3)$$

We can now define an improvement factor I_{ME} in the detectable minimum magnet diameter over the unoptimized case (CE=1, $R_{\mathrm{mag},u}$, $R_{\mathrm{sub},u}$, $D_{\min,u}$),

$$I_{\mathrm{ME}} = \frac{D_{\min}}{D_{\min,u}} = \sqrt{\mathrm{CE}\frac{R_{\mathrm{mag}}}{R_{\mathrm{mag},u}}\frac{R_{\mathrm{sub},u}}{R_{\mathrm{sub}}}}. \quad (4)$$

The largest improvement in sensitivity results if all three terms are maximized. As discussed above, the first two are related and work in opposite directions, leading to an ultimate limit in far-field MOKE enhancement. For the parameters of the previous SiN-coated magnets, we find $I_{\mathrm{ME}}=4.1$, in excellent agreement with the measured data. For the case of bare nickel magnets on an AR-coated substrate, we obtain $I_{\mathrm{ME}}=13$, which is somewhat larger than the experimentally observed value of $I_{\mathrm{ME}}=7.5$ due to the reasons described above. Nonetheless, this comparison shows that a good antireflection coating has a more dramatic effect on the MOKE signal than the CE layer. Finally, for the combined case of CE=5 (SiN) and a 0.2% AR coating, one can achieve $I_{\mathrm{ME}}=29$, corresponding to an improvement in areal sensitivity by about three orders of magnitude.

In summary, we analyzed and demonstrated optimization strategies of MOKE enhancement for nanomagnet studies. We found that better results are expected from the dual layer structure and the AR coating on the substrate is very efficient. Better spatial resolution and stronger Kerr signal were achieved in the quasistatic measurement of individual nanomagnets. Finally, an analytical expression for the limits of MOKE enhancement was presented, and three-order MOKE sensitivity improvement can be expected.

This work was supported by the National Science Foundation (Grant No. ECS-0245425) and the Office of Science, Office of Basic Energy Sciences, U.S. Department of Energy (Contract No. DE-AC02-05CH11231).

[1] S. K. Nair and R. M. H. New, IEEE Trans. Magn. **34**, 1916 (1998).
[2] G. A. Prinz, Science **282**, 1660 (1998).
[3] M. H. Kryder, J. Appl. Phys. **57**, 3913 (1985).
[4] K. J. Kirk, Contemp. Phys. **41**, 61 (2000).
[5] E. Beaurepaire, J. C. Merle, A. Daunois, and J. Y. Bigot, Phys. Rev. Lett. **76**, 4250 (1996).
[6] M. V. Kampen, B. Koopmans, J. T. Kohlhepp, and W. J. M. de Jonge, J. Magn. Magn. Mater. **240**, 291 (2001).
[7] Y. Acremann, C. H. Black, M. Buess, O. Portmann, A. Vaterlaus, D. Pescia, and H. Melchior, Science **290**, 492 (2000).
[8] J. P. Park and P. A. Crowell, Phys. Rev. Lett. **95**, 167201 (2005).
[9] A. Barman, V. V. Kruglyak, R. J. Hicken, A. Kundrotaite, and M. Rahman, Appl. Phys. Lett. **82**, 3065 (2003).
[10] K. S. Buchanan, X. Zhu, A. Meldrum, and M. R. Freeman, Nano Lett. **5**, 383 (2005).
[11] V. V. Kruglyak, A. Barman, R. J. Hicken, J. R. Childress, and J. A. Katine, Phys. Rev. B **71**, 220409(R) (2005).
[12] M. M. Noskov and A. V. Sokolov, Zh. Eksp. Teor. Fiz. **17**, 969 (1947).
[13] A. V. Sokolov, *Optical Properties of Metals* (Blackie, London, 1967), p. 311.
[14] K. Nakamura, T. Asaka, S. Asari, Y. Ota, and A. Itoh, IEEE Trans. Magn. **21**, 165 (1985).
[15] N. Qureshi, H. Schmidt, and A. R. Hawkins, Appl. Phys. Lett. **85**, 431 (2004).
[16] N. Qureshi, S. Wang, M. Lowther, A. R. Hawkins, S. Kwon, B. Harteneck, and H. Schmidt, Nano Lett. **5**, 1413 (2005).
[17] A. Barman, S. Wang, J. D. Maas, A. R. Hawkins, S. Kwon, A. Liddle, J. Bokor, and H. Schmidt, Nano Lett. **6**, 2939 (2006).
[18] G. J. Sprokel, Appl. Opt. **25**, 4017 (1986).